Chapter 4

Experimental Setup

The B_s oscillation analyses presented in this thesis were performed with the data sample collected by the ALEPH experiment between 1991 and 1995, during the phase 1 of LEP at CERN. A short reminder of LEP characteristics and achievements, in particular in its first running phase, are given to start this Chapter in Section 4.1. The ALEPH detector, one of the four multipurpose detectors of LEP, took data between August 1989 and November 2000. The detector and its performance for physics analyses are described in Section 4.2.

4.1 The LEP Storage Ring

The LEP [62] (Large Electron Positron Collider) storage ring is an e^+e^- collider located at CERN (European Laboratory for Nuclear Research). The LEP project was proposed in 1975, approved six years later, and started its operation in 1989. The main goal of the machine was to perform precision measurements of electroweak observables, in order to test the Standard Model at the level of radiative corrections. Such corrections take contributions from off-shell particles, and are therefore sensitive to physics beyond the production threshold. The LEP accelerator also provided the possibility to directly search for heavy, yet unobserved particles in a range of energies substantially higher than previous machines.

The accelerator programme consisted of two phases. In the first phase, LEP stored, accelerated, and collided electrons and positrons at a centre-of-mass energy around the Z boson mass (91.2 GeV), with a typical instantaneous luminosity of 10^{31} cm^{-2} s^{-1}. Several million of Z bosons were produced and their decays studied (as in the analyses described in this thesis). Since 1995, the centre-of-mass energy was increased every year. In 2000, the last year of running, a centre-of-mass energy of 209 GeV was reached, shortly before the machine was shutdown for the last time. The LEP dismantling started in November 2000.

The LEP ring is located underground, inside a nearly horizontal tunnel of 26.67 Km of circumference, at a depth which varies between 50 m and 150 m, spanning the French and Swiss territories (Fig. 4.1). The plane of the tunnel is inclined by 1.4% to ensure that all underground caverns and the main part of the tunnel are located in solid rock while, at the same time, the maximum depth of the shafts is limited to less than 150 m. The LEP accelerator consists of eight arcs alternated with eight straight sections. The beams are

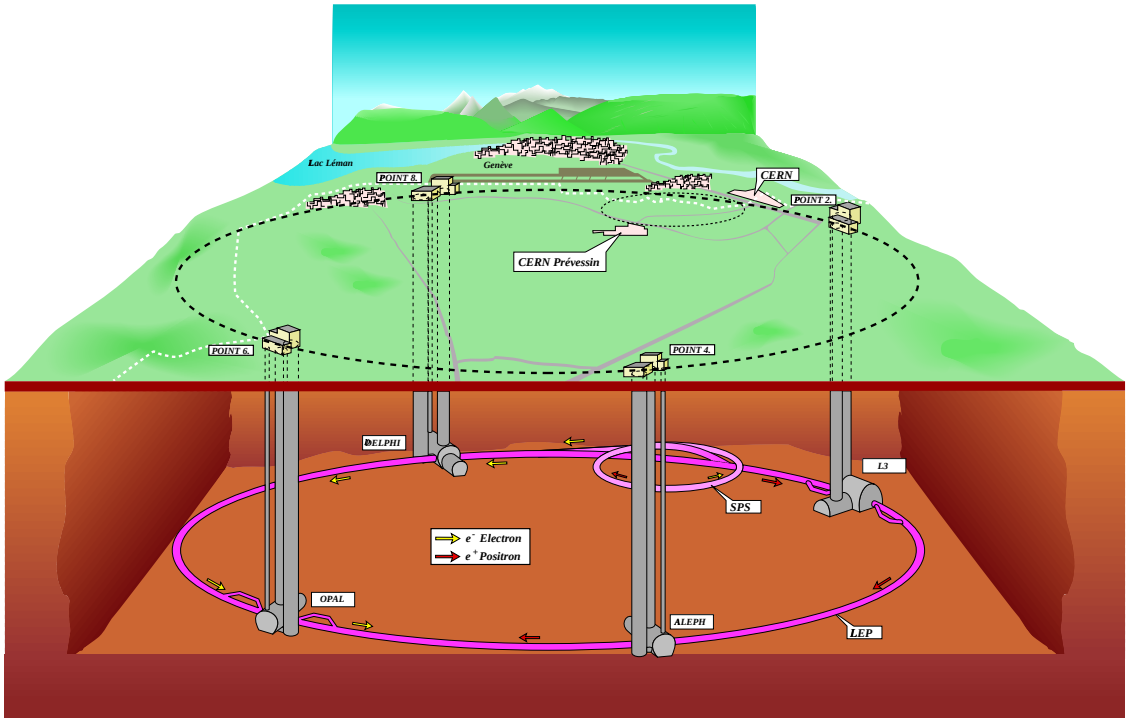

Figure 4.1: Schematic view of LEP and the Surrounding Area.

formed by bunches of electrons and positrons which circulate inside the beam pipe at nearly the speed of light for many hours (typically 10 hours at the Z, 1h30 at 207 GeV, and 15 minutes at 209 GeV). The beams are accelerated in opposite directions and cross in eight points, although they are steered to collide only on the four *Interaction Points* (I.P.). The straight sections, about 500 m long, are located around these eight points. The four LEP experiments, ALEPH, DELPHI, L3, and OPAL are sited in the middle of the interaction regions (Figs. 4.1 and 4.2).

The LEP injection chain can be seen in Fig. 4.2: it is formed by five accelerators, each of which handles the same electrons and positrons. Electrons are generated by the electron gun. A fraction is used to create positrons by collision with a tungsten target. Two linear accelerators (LINAC) of 200 MeV and 600 MeV are used to accelerate the lepton beams. Following the LINAC's, the particles are injected into a small circular electron positron accumulator, the EPA. They are then injected into the PS (proton synchrotron) accelerator, where the energy is increased up to 3.5 GeV. The PS injects the beams into the Super Proton Synchrotron (SPS), which operates as a 20 GeV electron-positron injector for LEP (since 1997, this energy has been increased up to 22 GeV). These last two machines (the PS and SPS), are operating at CERN since 1959 and 1976 respectively. Finally electron and positron beams are accelerated in LEP to reach the nominal energy.

The acceleration in LEP is provided by radio-frequency (RF) cavities and the magnetic

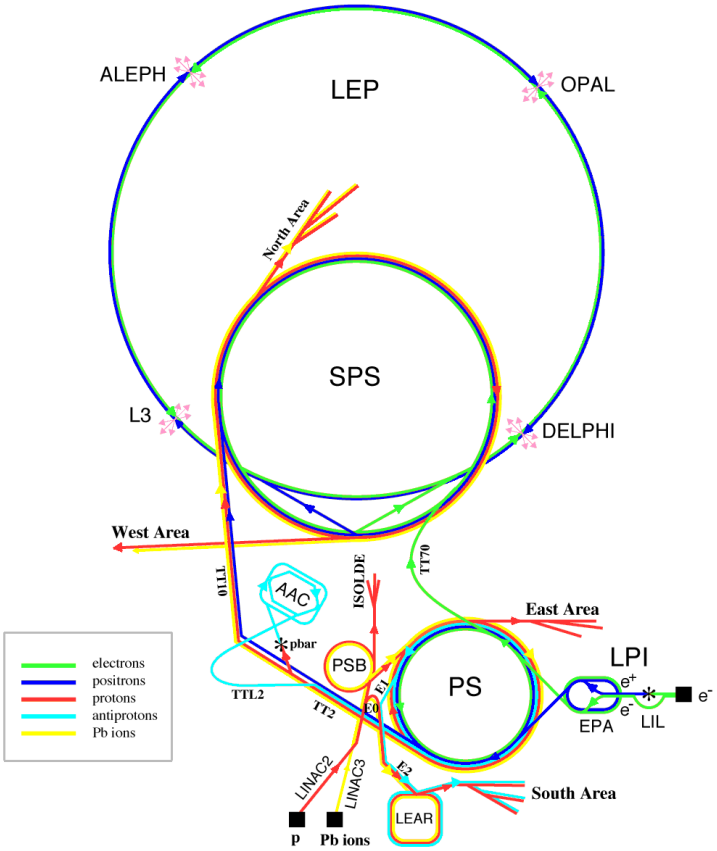

Figure 4.2: CERN Accelerators, LEP injection chain. The accelerators are not drawn at scale.

field. The RF system provides the energy needed to compensate for the synchrotron radiation loss in the curved trajectories, while the magnetic field is used to increase the energy from the initial $\sim 20\,\mathrm{GeV}$ to the nominal energy.

The performance of an accelerator is expressed with the centre-of-mass energy at which the collisions are made, and with the *luminosity* achieved. The luminosity is a quantity which relates the interaction rate for a given process to its cross-section:

$$\frac{dn}{dt} = \sigma \mathcal{L} \tag{4.1}$$

where dn/dt is the production rate of events according to the corresponding cross-section σ for a luminosity $\mathcal{L}$. The *luminosity* is defined by equation 4.1.

The luminosity provided by a collider can be expressed and computed in terms of its parameters. Therefore, if these parameters are known, the expected luminosity can be computed. The corresponding expression in the case of a circular collider like LEP is [63]

$$\mathcal{L} = \frac{k_b \; I_{\mathrm{e}^+} I_{\mathrm{e}^-}}{4\pi \; e^2 \; f_{\mathrm{rev}} \; \sigma_x^* \; \sigma_y^*} \; , \tag{4.2}$$

where k_b is the number of bunches per beam, I_{e^+}, I_{e^-} are the electron and positron beam currents, f_{rev} is the revolution frequency of the beam collisions, and σ_x^*, σ_y^* are the widths

of the Gaussian distributions representing the r.m.s. beam sizes at the collision point (it is assumed that the current intensity can be expressed as, $I = Nef_{\mathrm{rev}}$, e being the electric charge, and N the number of electrons). Typical values for the instantaneous LEP luminosity which can be obtained with this expression are of the order of $10^{31}\,\mathrm{cm}^{-2}\mathrm{s}^{-1}$, in agreement with the actual LEP performance at its first phase.

The total luminosity delivered by LEP to the four experiments in each of the 12 years of running is shown in Fig. 4.3. The integrated luminosity delivered at the Z pole from

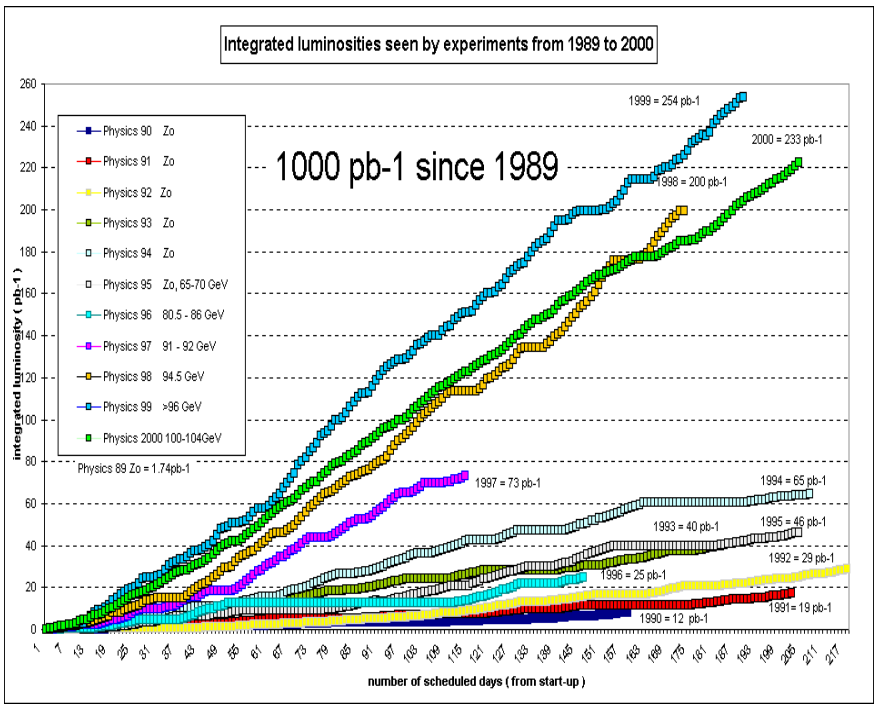

Figure 4.3: LEP Integrated luminosity from 1989 to 2000.

1991 to 1995 is $\sim 190\,\mathrm{pb}^{-1}$. During the second phase of LEP, some luminosity was also delivered at the Z pole, this data was mostly foreseen for detector calibration purposes. It is not included in the data sample analysed for the present thesis. Some parts of the ALEPH detector (mainly VDET, see Section 4.2.1) were upgraded for the second LEP phase, and therefore the analysis of the additional Z data requires specific studies. This fact, together with the relatively small fractional increase in statistics ($\sim 10\%$), discouraged the analysis of the additional Z decays.

4.2 The ALEPH Detector and Performance

The ALEPH (Apparatus for LEP Physics) detector, is one of the four experiments at the LEP collider of CERN. It is located at the interaction point number four in a cavern at 143 m under the surface. The approximated shape of the apparatus is a 12 m diameter by 12 m length cylinder positioned around the LEP beam pipe. Its axis coincides with the beam axis

and it is parallel to the magnetic field. It covers as much of the 4π solid angle as possible. It is designed to measure the momenta of charged particles, to measure the energy deposited in calorimeters by charged and neutral particles, to identify the three lepton flavours, and to measure the distance of travel of short-lived particles such as the tau lepton and the b and c hadrons. Particular emphasis has been given to momentum resolution up to the highest energies (by means of a large tracking system in a magnetic field), to electron identification (by means of a highly segmented, projective electromagnetic calorimeter, as well as ionization measurement in the tracking system), and to muon identification (with continuous tracking inside sufficient iron absorber to eliminate the hadrons).

In the ALEPH reference system, the z-direction is tangent to the beam pipe, positive in the direction followed by the electron beam. The positive x-direction points to the centre of the LEP ring and the positive y-direction is orthogonal to z and x (pointing to the top). A sketch of the detector with all the subdetectors shown is displayed in Fig. 4.4.

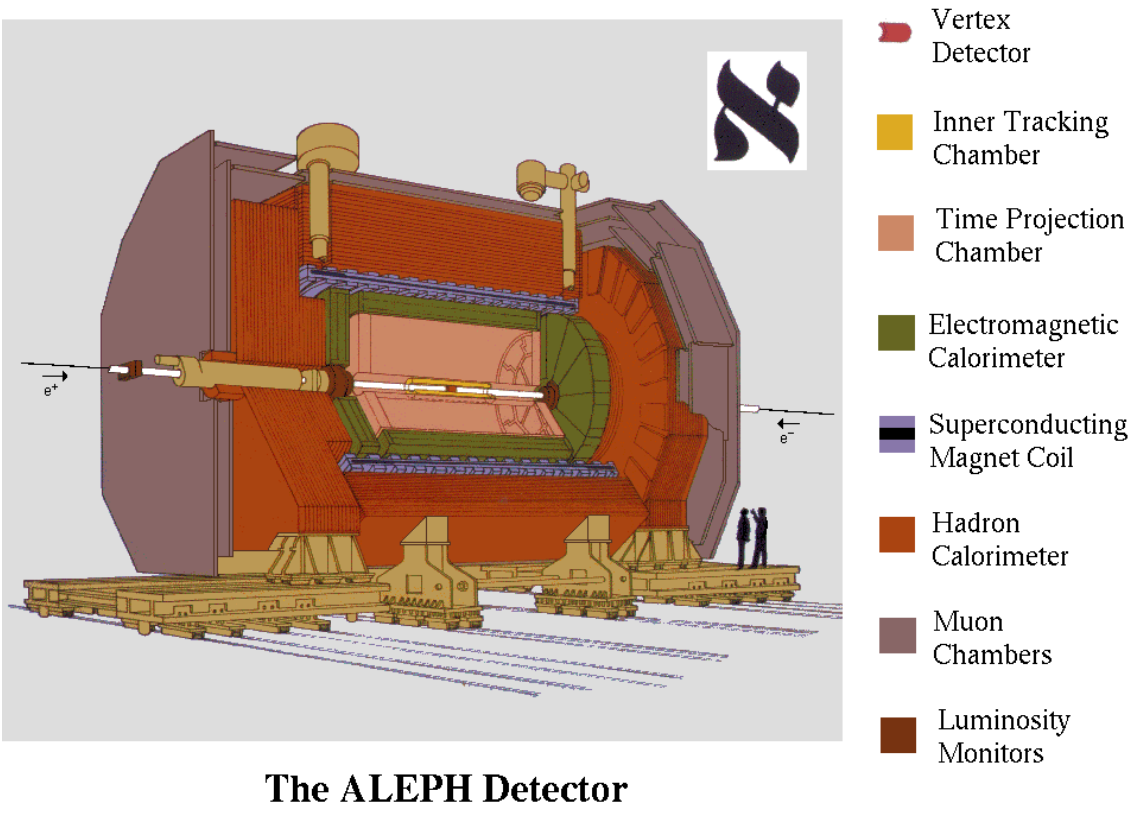

Figure 4.4: Schematic view of the ALEPH Detector, with all sub-detectors.

The ALEPH detector is described in details in Refs. [64] and [65], and its performance in Ref. [66]. Here only a brief discussion is presented, with particular emphasis on the aspects most relevant for the analysis described in this thesis.

4.2.1 The tracking system

The tracking system of a particle detector aims at reconstructing charged particles trajectories inside the system (tracks). It is a non-destructive system, which most of the particles traverse with almost no variation on their momentum. In some cases (if immersed in a magnetic field), it is also capable of separating positively from negatively charged particles, and to some extent, to provide particle identification.

The ALEPH tracking system involves three detectors. From the inner to outer part those are, the vertex detector (VDET), the inner tracking chamber (ITC) and the time projection chamber (TPC). They are immersed on a 1.5 T axial magnetic field created by a super conducting solenoid. In an axial and uniform magnetic field, B, charged particles have helix trajectories with a curvature, ρ, proportional to their transverse momentum, p_T, as

$$p_T \;=\; q\rho \mathrm{B}\;, \tag{4.3}$$

where q is the electric charge of the particle. The electric charge sign of reconstructed particles is given by the rotation sense.

The vertex detector

The ALEPH silicon vertex detector (VDET) was installed in 1990 and was fully operational in 1991. It provides high-precision measurements of charged particles trajectories close to the interaction point, without which the analyses presented in this thesis would not be possible.

The configuration of the VDET is shown in Fig. 4.5. Two layers of silicon strip detectors

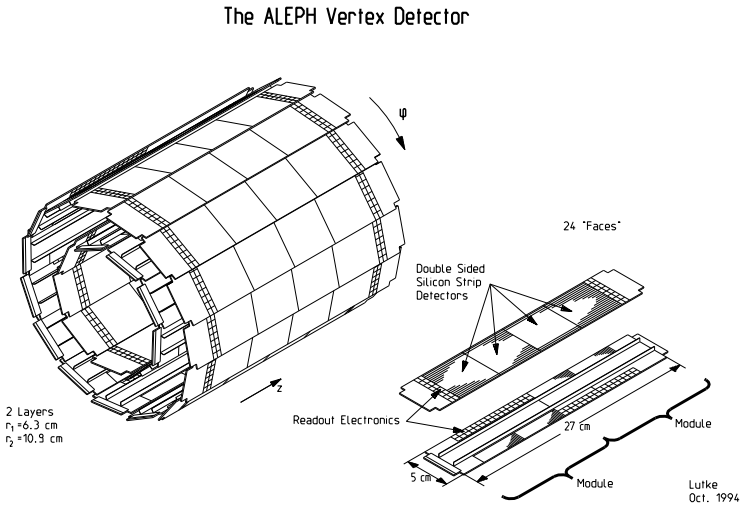

Figure 4.5: Configuration of the vertex detector.

are arranged in two concentric barrels around the beam pipe, with an average radius of $r_1 \approx 6.3\,\mathrm{cm}$ for the inner layer, and $r_2 \approx 10.9\,\mathrm{cm}$ for the outer layer. The strips on one side are parallel to the beam direction and measure the azimuthal angle ϕ. The strips on the other side are perpendicular to the beam and measure the z-coordinate. The radius, r, of the

individual wafers is given by the mechanical holding frame. The position of a single particle hit is then determined in cylindrical coordinates, $(r\,,\phi\,,z)$.

The vertex detector hits are used to improve the precision of the track reconstruction obtained with the outer tracking. The overall tracking performance is given at the end of this Section. The effective point resolution achieved by the vertex detector alone in both directions, $r\,\phi$ and $r\,z$, is $\sim 12\,\mu$m. The VDET solid angle coverage is 87% and 70% for the inner and the outer layers respectively.

The first-generation ALEPH vertex detector pioneered the use of double-sided silicon microstrip technology. In autumn 1995 it was replaced by an upgraded longer version which provides better solid-angle coverage and more radiation resistance. All the data analysed for this thesis were obtained before the vertex detector upgrade.

The Inner Tracking Chamber

The inner tracking chamber (ITC) is a cylindrical multiwire drift chamber which provides up to eight accurate $r\,\phi$ points for tracking in the radial region between 16 cm and 26 cm and $|\cos\theta| < 0.99$. As a fast response device, with a reaction time within $1\,\mu$s$-3\,\mu$s, it also provides the only tracking information used for the first-level trigger.

The wires run parallel to the beam direction in a gas mixture made of 80% argon and 20% carbon dioxide at atmospheric pressure. The $r\,\phi$-coordinate is obtained from the drift time measurement. A precision of about $150\,\mu$m is achieved. The z-coordinate is found with the measurement of the difference in the arrival times of pulses at the two ends of each sense wire with a coarse precision of about 5 cm.

The Time Projection Chamber

The time projection chamber (TPC) is the most important element of the ALEPH tracking system. It was chosen for its good momentum and angular resolution capabilities, as well as its ability for particle identification through the $\mathrm{d}E/\mathrm{d}x$ (energy loss by ionization in matter) measurements of charged particles. The chamber has a cylindrical structure, as shown in Fig. 4.6. It is 4.7 m long, with 0.31 m inner radius and 1.8 m outer radius. The chamber is divided in two halves by a high voltage central membrane which produces the longitudinal electric drift field. It is filled by a mixture of argon (91%) and methane (9%) at atmospheric pressure. The closing end-plates are covered by wire chambers organized in "sectors". Charged particles, when traversing the chamber, produce electrons by ionization of the gas. These electrons drift towards one of the closing end-caps, where they are collected. Their arrival position and time are measured by the wire chambers and pads. The z-coordinate is obtained from the drift time and the known drift velocity. The ϕ-coordinate is calculated by the interpolation of the signals induced on cathode pads located on the sectors and the r-coordinate is given by the radial position for the pads involved in the measurement. The chamber measures 21 three-dimensional points for each charge particle traversing the inner and outer field cages.

The azimuthal coordinate resolution obtained with leptonic Z decays is $\sigma_{r-\phi} = 173\,\mu$m. The longitudinal resolution is $\sigma_z = 740\,\mu$m for charged particles close to normal incidence,

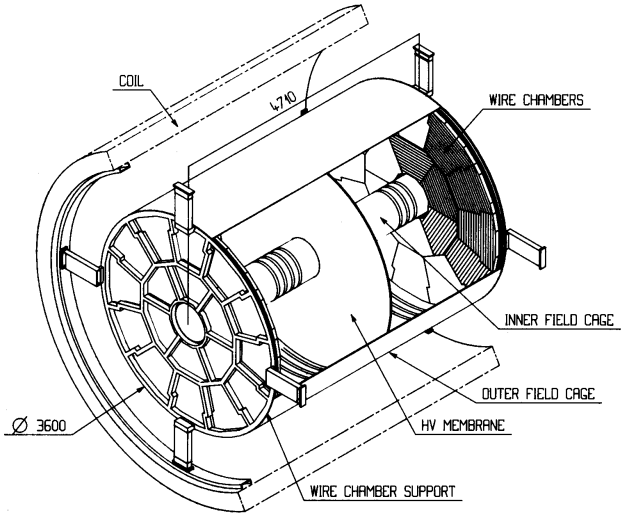

Figure 4.6: Time projection chamber overall view.

$80^\circ < \theta < 100^\circ$.

The ALEPH data from the LEP1 phase were reprocessed in 1998. The reason for this reprocessing was to implement improvements on the track reconstruction [67] and to include new information on $\mathrm{d}E/\mathrm{d}x$ measurement from the TPC. Only the wires measurements used to be available, but the less accurate pads measurements are now used as well. A complete description of the new $\mathrm{d}E/\mathrm{d}x$ combination algorithm and performance can be found in an ALEPH internal note [68].

Tracking performance

All three detectors are used for the track reconstruction in ALEPH. The reconstruction algorithm uses the TPC information first. Close hits (measured three-dimensional points) are linked together to from track segments, and the segments are connected to make tracks by requiring consistency with a helix hypothesis. These track candidates are extrapolated to the inner detectors, ITC and VDET, where consistent hits are assigned. The final track fit takes into account multiple scattering between subsequent points.

The overall performance of the momentum measurement for charged particles with full tracking information is shown in the first column of Table 4.1. The performance obtained with the TPC alone is presented first, followed by the effect of the other two devices. The TPC momentum resolution is improved by a factor two when the measurement is complemented with that of the other tracking devices.

The tracking system is also used for track impact parameter measurement (defined and used in Sections 5.5 and 5.7.1). The impact parameter resolution obtained on data for high momentum charged particles is also shown in Table 4.1 (second and third columns). The vertex detector is essential for the accuracy on the impact parameter measurement. When it

Detector	$\sigma(1/p_T)(\mathrm{GeV}/c)^{-1}$	$r\phi$ (μm)	rz (μm)
TPC	1.2×10^{-3}	310	808
+ ITC	0.8×10^{-3}	107	808
+ VDET	0.6×10^{-3}	23	28

Table 4.1: Momentum (first column), and impact parameter resolution performance. The successive rows show the improvement obtained when the detectors are successively included in the track fit.

is used, the resolution is reduced by more than an order of magnitude.

The ALEPH tracking system has achieved very good performance, without need of too much material which would degrade the final energy measurement. In Fig. 4.7 the thickness of the materials traversed by particles is expressed as a percentage of a radiation length, summed over the various materials traversed. It has a strong dependence on the polar angle θ, especially at small θ where the incidence into the material is oblique (because the material is often arranged in cylindrical layers).

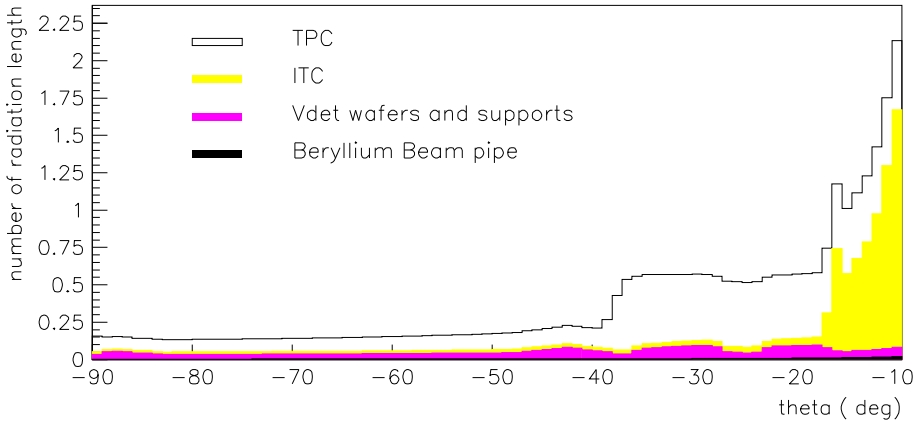

Figure 4.7: Material before the electromagnetic calorimeter measured in number of radiation length.

4.2.2 Calorimetry

Calorimeters are devices which measure the energy of particles by stopping them in a dense material. Characteristic interactions with matter (*e.g.*, atomic excitation, ionization) are used to generate a detectable effect, via charged particles, which is then translated to an energy measurement. Different types of particles have different penetration power in matter. In particular electrons and photons are easily absorbed, unlike hadrons. An electromagnetic calorimeter is meant to be able to stop electrons and photons, while hadrons typically traverse it leaving only a fraction of their initial energy. It is therefore common, like in ALEPH, to build a hadron calorimeter outside the electromagnetic calorimeter. Muons, as minimum ionizing particles, have an even higher penetration power than hadrons and are not stopped after the two calorimeters; the muon chamber detectors are located at the most external

part of ALEPH to detect their presence. Neutrinos almost do not interact with matter, the ALEPH detector is blind to them.

The Electromagnetic calorimeter

The electromagnetic calorimeter (ECAL) is located between the TPC and the magnet. It is a lead/wire-chamber sampling calorimeter, which measures the energy and position of electromagnetic showers from electrons and photons. Its nominal thickness is 22 radiation lengths (X_0).

The geometrical structure of the detector is approximately cylindrical. The calorimeter consists of a barrel part, closed by flat end-caps. This structure and positioning with respect to the coil and the hadron calorimeter is shown in Fig. 4.8. The barrel is 4.8 m long, and

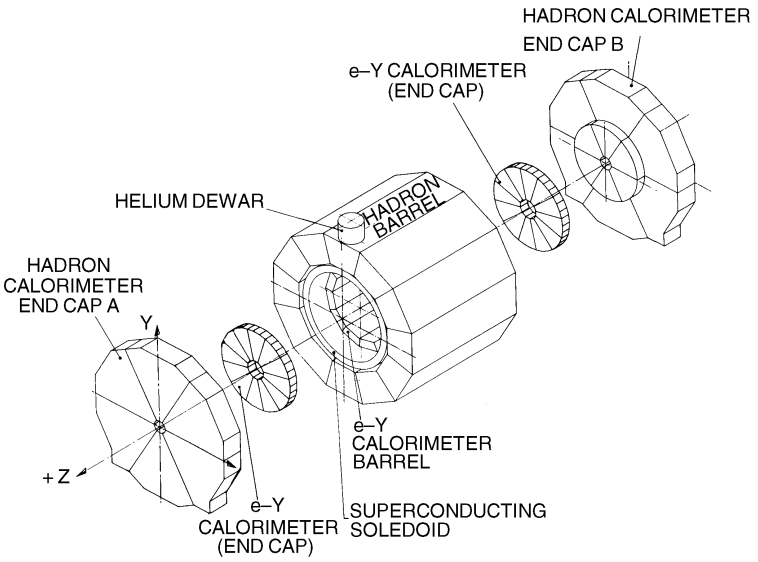

Figure 4.8: Overall geometry of the hadron calorimeter surrounding the superconducting coil and the electromagnetic calorimeter.

its inner radius is 1.54 m, while the outer is 2.53 m. Both end-caps and the barrel consist of 12 modules each. Each module is subdivided in towers pointing towards the centre of the detector. Each of the towers is read in three different depth modules called "storeys". The ensemble of storeys at the same depth is called a "stack". A total of 73728 towers provide a fine granularity of $0.9^\circ \times 0.9^\circ$ (in the barrel), which is very useful for $e/\gamma/\pi^0$ identification, energy, and angular measurement. The entire calorimeter is rotated by -32.7 mrad with respect to the hadron calorimeter to avoid overlapping of uninstrumented separation between modules (cracks). The polar angle coverage is $|\cos\theta_{\rm track}| < 0.98$.

The energy resolution for isolated electrons and photons, determined by comparing the measured energy to the track momentum, is fit to be

$$\frac{\sigma(E)}{E} = \frac{0.18}{\sqrt{E/\mathrm{GeV}}} + 0.009 \; . \tag{4.4}$$

The position of a shower is calculated by an energy-weighted mean of the polar and azimuthal angle of the individual storeys in the cluster. The spatial resolution is evaluated to be

$$\sigma_{\theta,\,\phi} = \left(\frac{2.5}{\sqrt{E/\mathrm{GeV}}} + 0.25 \right) \text{ mrad} . \tag{4.5}$$

The hadron calorimeter and the muon chambers

The hadron calorimeter is located inside a large iron structure which is the main mechanical support of ALEPH and which also serves as a return yoke for the magnetic flux. The iron plays the rôle of the passive material in a sampling calorimeter, while the active part is provided by layers of plastic streamer tubes. The HCAL is used as a muon filter as well as a powerful muon identification tool. It also measures the energy of neutral and charged hadrons which are not stopped in the electromagnetic calorimeter.

As seen in Fig. 4.8, the hadron calorimeter is subdivided in a central barrel and two closing end-caps. The total thickness of the iron is 1.2 m, which amounts to 7.16 interaction lengths for a hadron traversing the calorimeter perpendicular to the slabs.

The energy resolution for pions at normal incidence, when both ECAL and HCAL are used, is found to be:

$$\frac{\sigma(E)}{E} \approx \frac{0.85}{\sqrt{E/\mathrm{GeV}}} . \tag{4.6}$$

Part of the hadron calorimeter readout is used for muon identification (see Section 5.3.2). In addition, two layers of muon chambers are placed outside the hadron calorimeter. Each of these chambers is made of two layers of streamer tubes which are not used here for energy measurement, but as tracking devices for the detection of particles leaking out the hadron calorimeter. The two layers are separated from each other by a sufficient distance so that not only the position but also the angle of a charged particle can be measured. Up to two three-dimensional coordinates are then obtained for each charged particle traversing a muon chamber.

4.2.3 Energy flow

The energy flow algorithm [66] combines the energy and particle identification measurements from the calorimeters and the tracking system. The overall energy measurement is therefore significantly improved.

As a first step, "good" tracks (with a similar selection as the one described in Section 5.1) are identified, and extrapolated to the two calorimeters. The energy deposits around the extrapolated tracks are associated to them. The calorimetric objects are then formed by these charged particles and calorimetric deposits or energy deposits in the ECAL associated with energy deposits in the HCAL. The calorimetric objects are then treated in the following manner:

- Tracks identified as electrons, with their associated deposits in the ECAL are eliminated from the calorimetric objects list. If the difference between the calorimetric energy

and the track momentum is greater than 3 times the ECAL resolution, this energy difference is taken as coming from a Bremsstrahlung photon, and counted as a neutral electromagnetic object.

- Tracks identified as muons are eliminated from the list as well, together with the energy of the associated calorimetric cluster, with a maximum energy of 1 GeV in the ECAL and 400 MeV per HCAL layer in the extrapolated 'road'.

- Photons are eliminated from the calorimetric objects list as well, and are counted as neutral electromagnetic objects.

- Only charged and neutral hadrons remain in the calorimetric objects list. The charged particles and their associated calorimetric objects are eliminated from the list. The remaining calorimetric energy is considered as coming from neutral hadronic particles.

4.2.4 Luminosity measurement

The luminosity received by the ALEPH detector is determined from the reconstruction of small angle elastic e^+e^- scattering (the so-called Bhabha scattering) in a well defined fiducial region. The Bhabha scattering at low angle is a purely QED process and its cross-section can be calculated with high precision. To a good approximation it amounts to,

$$\frac{d\sigma_0}{d\Omega} \simeq \frac{4\alpha^2}{E_b^2\,\theta^4}\ , \tag{4.7}$$

where α is the fine structure constant, E_b is the beam energy, and θ is the polar scattering angle of the electron or positron with respect to the beam direction.

Three lumonisity detectors were in use by the end of the experiment life. The ALEPH luminosity measurement was performed up to 1991 by a specific electromagnetic calorimeter called LCAL. The detector structure is very similar to that of the ECAL. The LCAL is located around the beam pipe on both sides of the interaction region with the first sampling layer at a distance of 2.63 m from the I.P. The detector covers, in the horizontal plane, a polar angle range of $45\,\text{mrad} < \theta < 160\,\text{mrad}$. With this detector the accuracy obtained on the luminosity measurement was of, at best, 0.4 %, which was found not to be enough for the needs of some physics analyses (in particular the Z line-shape studies [69]). It was therefore decided to build and install a new more precise luminosity detector: SiCAL.

The silicon luminosity calorimeter (SiCAL) [70], installed in 1992, consists of two homogeneous cylindrical silicon-tungsten sampling electromagnetic calorimeters which surround the beam pipe at approximately $z = \pm 2.5\,\text{m}$ on either side of the interaction point. The active volume of the detector subtends the polar angular region, $24.3\,\text{mrad} < \theta < 57.5\,\text{mrad}$. The aim of SiCAL was to reduce the total uncertainty in the luminosity measurement down to 0.1%. The SiCAL polar angular coverage is closer to the beam pipe than that of LCAL, to improve the statistical precision. A greater accuracy, with respect to LCAL, in the determination of the position of the detector components allowed the fiducial cross-section estimation to be improved, and therefore the systematic uncertainty on the luminosity measurement was reduced.

For the LEP2 phase, SiCAL was not used as the luminosity monitor anymore. The photon synchrotron radiation having increased dramatically compared to LEP1, new "masks" were installed close to the beam pipe to protect the central sub-detectors. These elements were added on the region where the SiCAL modules were positioned and their shadow reduced the fiducial region which could be used for the Bhabha rate counting below the needs for providing a measurement accurate enough.

The third luminosity detector, BCAL, is used for an online monitoring of the instantaneous luminosity. The two previous detectors could not be used for this purpose because their event rates are too low for a reliable and quick online estimate of the luminosity. The BCAL monitor consists of four modules (sampling calorimeter made of tungsten, scintillator and silicon) located very close to the beam pipe and more than 7 m from the interaction point, to detect Bhabha events at very small angle. The first version of the detector, which was in use till 1996, had a polar angle coverage of $5.1\,\text{mrad} < \theta < 9.0\,\text{mrad}$. The second version installed in 1997 was able to cover angles down to $\approx 4.5\,\text{mrad}$. The uncertainty on the online luminosity was about 5% (every two minutes) for a luminosity of 10^{31} cm^{-2}s^{-1}.